11

Synthesis of L-band diplexer for high power operation

© K.V. Kobrin, M.B. Manuilov

Southern Federal University,
344090 Rostov-on-Don, Russia
e-mail: m_manuilov@sfedu.ru

Received December 28, 2023
Revised December 28, 2023
Accepted December 28, 2023

The efficient combined technique is proposed for synthesis of L–band diplexer for high power operation which is necessary, for example, in radar applications. The original diplexer modification is implemented on the base of coaxial cavity resonators with the jump of characteristic impedance. The suggested mushroom design of coaxial resonator provides the compact size due to reducing the electric length of resonator and it is appropriate for high-power operation. The original design of the coaxial-to-strip-line bifurcation is introduced into diplexer as the matching circuit. Synthesis technique of diplexer includes the application of the coupling matrixes technique, solving the eigen-value problems for single resonator and two coupled resonators, full-wave simulation based on finite element technique. As a result of synthesis high electrical performances of diplexer were obtained. Within frequency bands of diplexer 1024−1036/1084−1096 MHz the reflection coefficient is less than $S_{11} < -22$ dB, the channels isolation is better -70 dB, insertion loss is -0.4 dB, maximal operational power is 2 kW. The proposed design of diplexer is appropriate for implementation within the operational frequency bands of mobile and satellite communications.

Keywords: Diplexer, band-pass filter, coaxial resonator filter, coaxial-to-strip-line transition, coupling matrix, scattering matrix, eigen-value problem.

DOI: 10.21883/0000000000

Introduction

Diplexers are a basic element of various communication and radar systems, in which they are used to frequency separate transmission and reception channels. The diplexer contains two channel band-pass filters and a matching circuit, which makes it possible to receive and transmit signals using one antenna. In this case, there is a strong electromagnetic interaction between the channel filters, which significantly complicates the task of designing this class of devices. The key parameters when designing diplexers are insertion loss, channel isolation, matching, permissible power level, intermodulation distortion, and device dimensions. Low insertion loss in the reception path is important because it reduces the overall noise figure in the reception path. In the transmission path, the amount of losses is also important, since the energy efficiency of the system depends on it. The required level of isolation of the transmitting and reception paths prevents the leakage of a powerful signal from the transmitter into the reception path. Thus, in each case, the electrodynamic design of diplexers is a search for a compromise between insertion losses, channel isolation, alignment and device dimensions.

The choice of diplexer structure and type of resonant cavities is determined by the operating frequency ranges and the requirements for electrical and other characteristics, which depend on the specific applications. Diplexers based on coaxial resonators of various types [1–6], on interdigital resonators [7–11], on dielectric resonators [1,12–15], strip-line [16] and waveguide structures [17] are widely used in wireless communication systems.

Various designs of diplexers and filters on coaxial resonators are used mainly in the radio frequency range [1–6]. The advantages of this type of structure are low insertion losses, flexible options for implementing characteristics with wide, medium and narrow pass bands and high power operation. Currently, research is being carried out for this class of devices aimed at improving their design and developing synthesis methods. The disadvantage is the relative complexity of the design.

Modern developments in the field of high-quality dielectric materials have ensured success in the creation of diplexers and filters on dielectric resonant cavities, in which it is possible to realize high values of unloaded quality factor [12–15]. Frequency-selective structures based on dielectric resonant cavities are used in mobile and satellite communication systems. However, the disadvantages of these structures include higher losses than in filters based on resonant cavities.

The current task is to develop diplexers for mobile communication base stations. In particular, in [7–9] new designs of diplexers based on interdigital resonators are proposed, and in [16] — new stripline designs of filters and diplexers for use in antennas of mobile communication base stations. In addition to frequency separation of transmission and reception channels in the antennas of mobile communication base stations, diplexers are used to implement multi-band operation (dipole reuse technology). The diplexers proposed in [7–9,16] provide low insertion loss (0.2−0.5 dB)

in the transmittance band, low intermodulation distortion, and have a compact technological design suitable for mass production.

Let us note that structures on interdigitated resonant cavities using modern technologies (additive technologies, 3*D*-printing) [10,11] are implemented and used in the centimeter and millimeter ranges, which allows them to be considered as a basic element for use in mobile communication systems 5G. Waveguide diplexers are most widely used in the centimeter and millimeter ranges; for example, in [17] a new compact modification of the waveguide diplexer was proposed on ridge sections and longitudinal diaphragms in the *E*-plane of waveguide.

This work considers the problem of synthesizing an *L*-band diplexer to operate at a high power level, which is relevant, for example, in air traffic control radar systems. Based on the set of requirements, a modified design of a diplexer based on coaxial resonant cavities and a combined method for its synthesis are proposed below.

1. Diplexer design

When setting up the problem, it was assumed that the operating bands of the diplexer are 1024–1036/1084–1096 MHz, the maximum power is 2 kW, the channel isolation should be no worse than −60 dB, the diplexer should have low insertion losses and high matching. The diplexer ports are standard 50 Ohm high power coaxial connectors (*N*- type).

Taking into account this set of requirements, the modified structure of the diplexer, shown in Fig. 1, was studied. A resonant cavity with a mushroom-shaped coaxial conductor is used as the basic element of channel filters. Each resonant cavity is a rectangular cavity with rounded corners in the metal housing of the diplexer. In the center of the cavity there is a coaxial conductor in the form of a hollow cylinder with an expansion in the form of a disk at the end, which corresponds to a jump in wave impedance. This choice of resonant cavity allows to significantly reduce the length of the coaxial cylinder for a given resonant frequency of the resonant cavity and avoid the appearance of narrow gaps with high field strength in the structure, which allows one to avoid electrical breakdown when operating at high power levels. In addition, each resonant cavity has a metal tuning screw, which is placed on a metal cover that covers the top of the diplexer body. When adjusting the resonant frequency, the screw can be immersed inside the hollow cylinder, which expands the tuning range of the resonant cavity.

The resonant cavities operate on a TEM wave and are interconnected by side coupling windows, each of which also has a metal tuning screw placed on the top metal cover of the diplexer. This number of tuning elements allows to quickly adjust the characteristics of the diplexer in the presence of manufacturing and assembly errors.

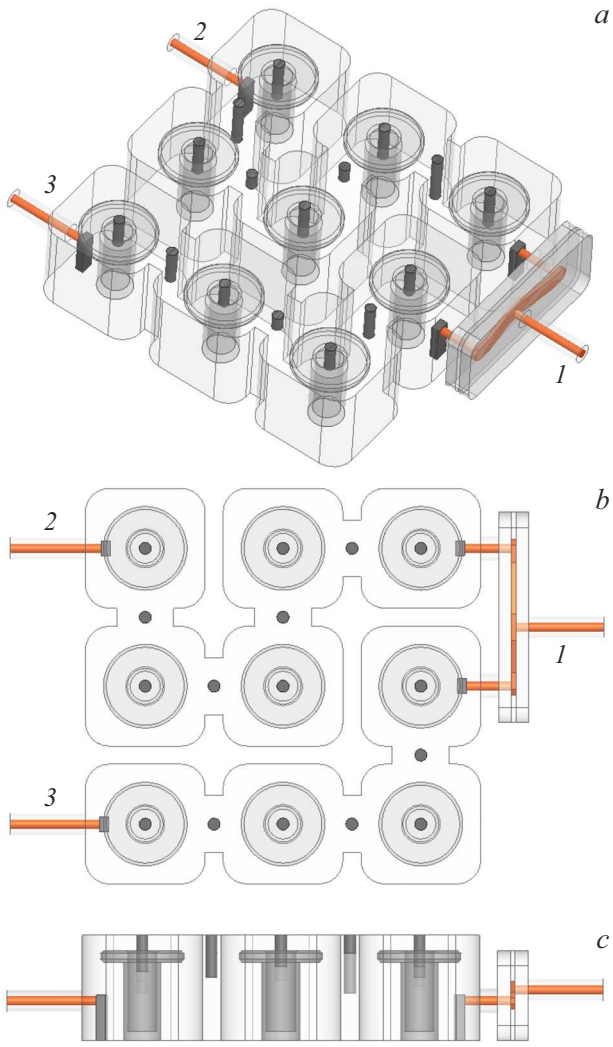

Figure 1. Three-dimensional model of diplexer for (*a*), top view (*b*), side view (*c*).

The excitation of the edge resonators in each filter is carried out using a magnetic coupling loop, implemented using vertical pins connected to the signal conductor of coaxial lines. The numbers *1*–*3* indicate the coaxial ports of the diplexer. Port *1* is connected to *T* by a branching of a symmetrical stripline with a characteristic impedance of 50 Ω, the shoulders of which are connected to the inputs of channel filters using 50-ohm coaxial lines.

Thus, the diplexer consists of a metal housing with resonant cavities, hollow coaxial cylinders that are attached to the housing with screws, a flat metal cover with tuning screws and a matching circuit based on *T*-bifurcation of strip line with coaxial-to-strip line transitions.

2. Synthesis method

The synthesis of the diplexer was carried out on the basis of a combined technique, including the following stages: (i) synthesis of channel filters based on coupling matrices;

(ii) solving the eigenvalue problem for a single and two coupled resonators; (iii) full wave optimization of channel filters obtained as a result of synthesis based on coupling matrices; (iv) diplexer full wave optimization.

Let us assume that channel filters have Chebyshev-type characteristics, and also set the maximum of reflection coefficient within the pass bands ($S_{11} < -20$ dB). Based on this, we determine the order of the filters ($n_1 = 5$ for the 1024−1036 MHz range, $n_2 = 4$ for the 1084−1096 MHz range).

Next, we will use the coupling matrices approach. A band-pass filter based on coaxial resonators can be represented as an equivalent scheme [1], where each resonators corresponds to an oscillatory circuit. The coupling matrix **M** has the dimension $n \times n$, where n — the number of resonators, and its element M_{ij} determines the coupling of resonators with numbers i, j. In the case under consideration, coaxial resonators operate on the main type of oscillations, which corresponds to the TEM wave of the coaxial line. Adjacent resonators are interconnected by coupling windows, and there is a strong electromagnetic interaction between them, which can be adjusted by the size of the coupling windows and the immersion depth of the tuning screw. The coupling with more distant resonant cavities will be much weaker, so in the coupling matrix we will take into account only the elements that describe the interaction of neighboring resonant cavities. Thus, we take into account the elements of the connection matrix, which are defined as follows [1,7]:

$$M_{j,j+1} = M_{j+1,j} = \frac{1}{\sqrt{g_j g_{j+1}}}, \quad j = 1, 2, \ldots, n-1, \quad (1)$$

$$R_1 = \frac{1}{g_0 g_1}, \quad R_n = \frac{1}{g_n g_{n+1}}, \quad (2)$$

where g_i — elements of the equivalent scheme of the prototype low-pass filter [18], and R_1, R_n — normalized impedances of the oscillator and load. The elements of the filter scattering matrix are determined taking into account (1), (2) by the following relations:

$$S_{11} = 1 + 2jR_1\left[w\mathbf{I} - j\mathbf{R} + \mathbf{M}\right]^{-1}_{11}, \quad (3)$$

$$S_{21} = -2j\sqrt{R_1 R_n}\left[w\mathbf{I} - j\mathbf{R} + \mathbf{M}\right]^{-1}_{n1}, \quad (4)$$

$$w = \frac{f_0}{\Delta f}\left(\frac{f}{f_0} - \frac{f_0}{f}\right),$$

where **I** — unit matrix of the n-th order; **R** — a matrix in which two elements $[\mathbf{R}]_{11} = R_1$, $[\mathbf{R}]_{nn} = R_n$, defined by expressions (2), are non-zero; f_0 — center frequency of the pass band; Δf — filter pass band.

From relations (1) for filter 1 (1024−1036 MHz, $n_1 = 5$) and filter 2 (1084−1096 MHz, $n_2 = 4$) we obtain the following coupling matrices:

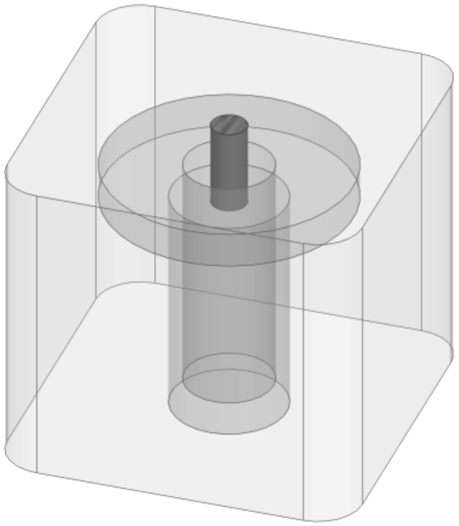

Figure 2. Single coaxial resonators (eigenvalue problem).

$$M_1 = \begin{pmatrix} 0 & 0.9068 & 0 & 0 & 0 \\ 0.9068 & 0 & 0.6533 & 0 & 0 \\ 0 & 0.6533 & 0 & 0.6533 & 0 \\ 0 & 0 & 0.6533 & 0 & 0.9068 \\ 0 & 0 & 0 & 0.9068 & 0 \end{pmatrix} \quad (5)$$

$$M_2 = \begin{pmatrix} 0 & 0.96 & 0 & 0 \\ 0.96 & 0 & 0.7268 & 0 \\ 0 & 0.7268 & 0 & 0.96 \\ 0 & 0 & 0.96 & 0 \end{pmatrix} \quad (6)$$

At the next stage, we solve the problem of calculating the resonant frequencies of the resonator. The formulation of the eigenvalue problem for a single coaxial resonator is shown in Fig. 2. The problem is solved by the finite element method in Ansys HFSS [19]. As a result of the simulation, the geometric dimensions of the resonator were found, which correspond to the central frequencies of the diplexer operating ranges of 1030 and 1090 MHz. A hollow coaxial cylindrical conductor with a diameter of 13 mm is placed in a resonant cavity with dimensions $40 \times 40 \times 35$ mm. The length of the coaxial cylinder is 30 mm, the diameter of the disk at the end of the cylindrical conductor is 28 mm. Thus, the gap between the end of the mushroom-shaped coaxial cylinder and the upper surface of the resonant cavity is 5 mm. Resonant cavities tuned to a frequency of 1030 or 1090 MHz have the same dimensions and differ in the depth of immersion of the tuning screw. When solving the eigenvalue problem, the dimensions of the resonant cavity were chosen in such a way as to achieve the maximum value of the intrinsic (unloaded) Q factor of the resonant cavity, since this allows to further ensure minimal insertion losses of the diplexer.

Next, it is required to calculate the dependence of the coupling coefficient between two adjacent resonant

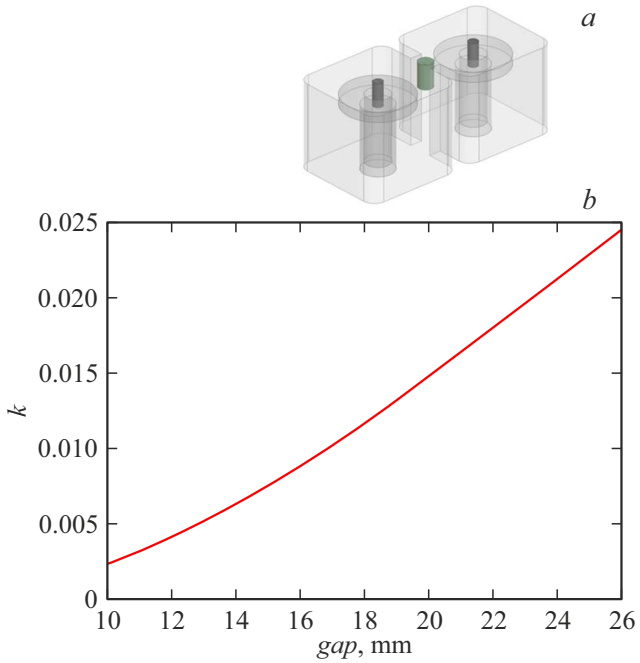

Figure 3. Calculation of the coupling coefficients of two resonators: formulation of the eigenvalue problem for two coupled resonators (a), dependence of the coupling coefficient on the width of the coupling window (b).

cavities on the geometric dimensions of the coupling window. For two coupled resonators shown in Fig. 3, a, the eigenvalue problem is solved and the coupling coefficient is calculated for different widths of the coupling window and a fixed length of the tuning screw. Since in the selected diplexer design (Fig. 1) the distances between the resonant cavities are the same, setting the connection between the resonant cavities is possible using the width of the coupling window and the immersion depth of the tuning screw. Figure 3, b shows the dependence of the coupling coefficient on the width of the coupling window at a fixed immersion depth of the adjusting screw equal to 10 mm. The magnitude of the coupling coefficient increases with increasing width of the coupling window and the immersion depth of the tuning screw.

Based on the obtained coupling matrices (5), (6) of the channel filters, we calculate the coupling coefficients for all resonators included in the filters:

$$k_{ij} = \frac{\Delta f}{f_0} M_{ij}.$$

For a five-resonant cavity filter 1 with an operating range of 1024–1036 MHz we obtain

$$k_{12} = k_{45} = 0.010565, \quad k_{23} = k_{34} = 0.0076118.$$

For a four-resonant cavity filter 2 with an operating range of 1084–1096 MHz, the coupling coefficients are equal

$$k_{12} = k_{34} = 0.010569, \quad k_{23} = 0.0080011.$$

Based on the calculated values of the coupling coefficients, we determine the sizes of the coupling windows in the filters using the dependence in Fig. 3, b.

3. Numerical results

The filter synthesis technique outlined above allows to calculate the frequency characteristics of diplexer channel filters using formulas (3), (4). In addition, the result of the synthesis at the first stage is the initial dimensions for constructing three-dimensional electrodynamic models of filters. At this stage, linear filter designs were considered, which were later transformed into more compact ones, taking into account the proposed diplexer structure in Fig. 1.

Figures 4, 5 show three-dimensional models of filters and their frequency characteristics, calculated using coupling matrices (3), (4) and in a rigorous full wave formulation using the finite element method in Ansys HFSS [18]. For a five-resonant cavity filter 1 (Fig. 4), there is a very good agreement between the characteristics calculated by the circuit theory using formulas (3), (4) and on the basis of a three-dimensional electrodynamic model — after numerical optimization of the filter. It should be noted that in the three-dimensional model (Fig. 4, a) in addition to the resonant cavities themselves, input coaxial waveguides with exciting vertical rods are added. For a four-resonant cavity filter 2 (Fig. 5), the characteristics synthesized using formulas (3), (4) and the characteristics of the three-dimensional electrodynamic model diverge somewhat more, since in the process of numerical optimization a higher agreement was achieved than in the approximate

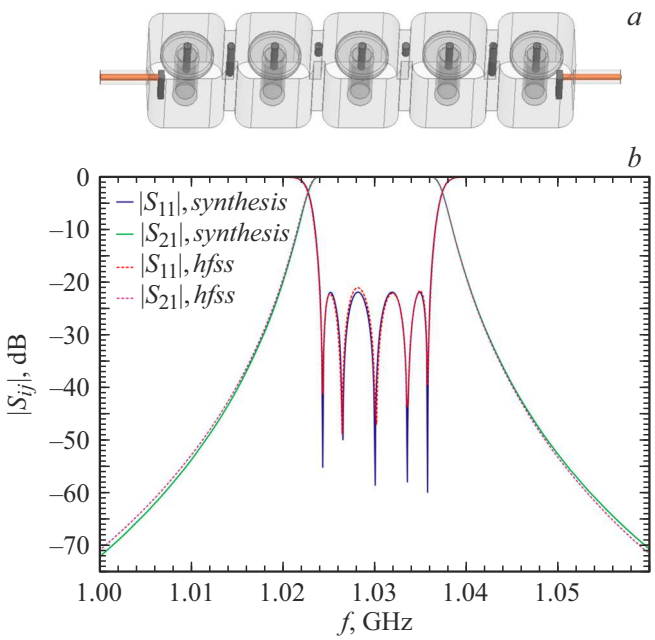

Figure 4. Filter band 1024–1036 MHz: three-dimensional model (a), frequency characteristics of the filter calculated as a result of synthesis and electrodynamic modeling (b).

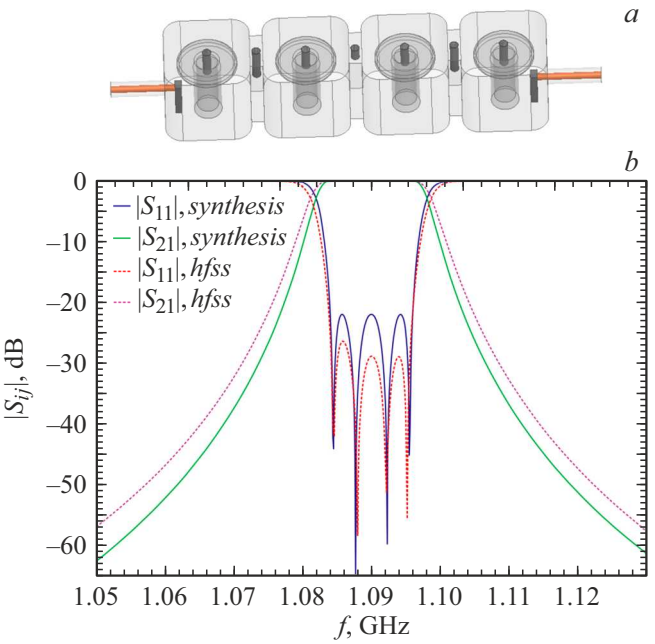

Figure 5. Filter band 1084–1096 MHz: three-dimensional model (*a*), frequency characteristics of the filter calculated as a result of synthesis and electrodynamic modeling (*b*).

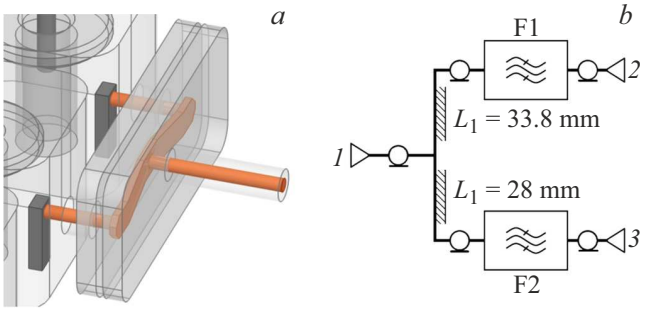

Figure 6. Matching circuit based on *T*-bifurcation (*a*) and block diagram of the diplexer in simulation based on circuit theory (*b*).

model. The width of the coupling windows between the resonant cavities and the length of the tuning rods in the resonant cavities and coupling windows were used as variable parameters when optimizing the characteristics of the filters. The remaining dimensions of all resonators remained unchanged during the modeling process.

Taking into account the requirement to operate at an increased power level, an original design of the diplexer matching circuit was proposed based on *T*-bifurcation of stripline with coaxial ports (Fig. 6, *a*). The center conductor of a symmetrical strip line is located in a rectangular cavity between two dielectric plates with dielectric permittivity $\varepsilon = 2.2$. The thickness of the plate is selected to ensure a threaded connection with the signal conductors of the coaxial lines. This design is technologically advanced and does not contain narrow gaps with high field strength, where there may be a risk of electrical breakdown.

To obtain an approximate estimate of the parameters of the matching circuit, the circuit theory was used. Fig. 6, *b* shows the corresponding block diagram of the diplexer, in which the channel filters are depicted in the form of blocks F1, F2. The previously calculated frequency characteristics of *S*-parameters of the filter are imported into the model in Fig. 6, *b* to describe the blocks corresponding to filters 1 and 2. As part of this approximate model, a single-mode approximation is used, i.e. the mutual coupling of higher modes between channel filters is not taken into account. An approximate calculation allowed to determine the dimensions of the *T*-joint as an initial approximation. The characteristic impedance of the strip line is 50 Ω, the arm lengths are 33.8, 28 mm.

A rigorous full wave calculation of the diplexer with the obtained initial dimensions shows that due to the presence of strong interaction between the channels, the characteristics of the diplexer are significantly degraded. Superimposed on Fig. 7 are the characteristics of the diplexer, calculated using circuit theory using a simplified

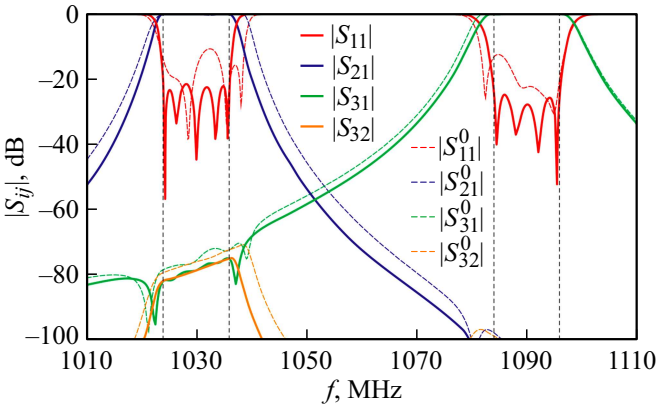

Figure 7. Frequency characteristics of the diplexer calculated based on circuit theory (solid lines) and the finite element method (dashed lines).

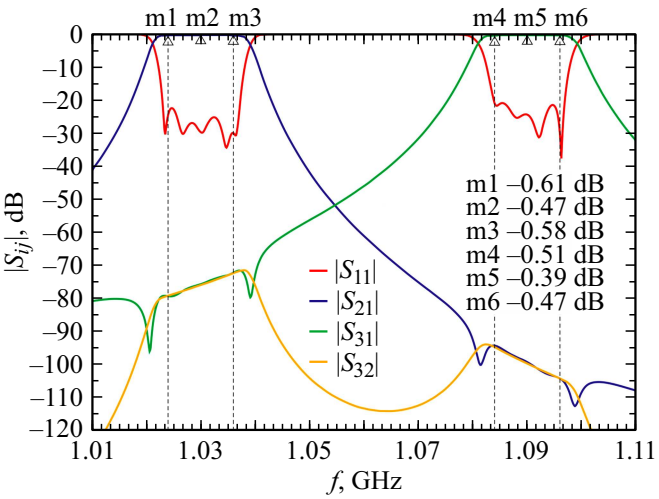

Figure 8. Frequency characteristics of the diplexer after electrodynamic optimization (labels indicate insertion loss values in dB).

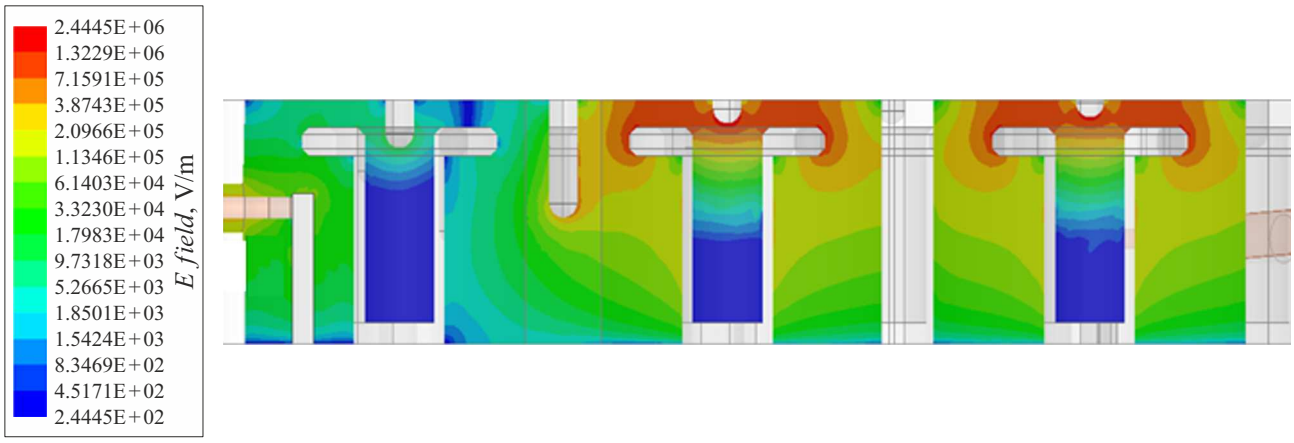

Figure 9. Distribution of electric field strength in a diplexer when 2 kW power is applied to its input 1.

model (Fig. 6, *b*) and the characteristics calculated by the electrodynamic method. The latter differ significantly from the characteristics calculated without taking into account the mutual connection of channels in terms of pass band, isolation, and the matching in the operating frequency band is significantly worse ($S_{11} > -10$ dB). Thus, further numerical optimization of the diplexer is required based on full-wave electrodynamic modeling.

As an initial approximation when carrying out multi-parameter optimization, the geometry of the diplexer was used, obtained on the basis of a simplified model in Fig. 6, *b*. The optimization parameter vector includes the sizes and positions of the rectangular rods connected to the coaxial ports, as well as the length of the tuning rods in the communication windows and resonant cavities. As a result of optimization, the diplexer characteristics shown in Fig. 8 were obtained. Diplexer pass band 1024–1036/1084–1096 MHz, reflection coefficient in pass band $S_{11} < -22$ dB (standing wave ratio SWR < 1.2), channel isolation $S_{32} = -70$ dB.

To estimate the insertion loss in the pass band, the conductivity of the silver coating of all internal surfaces of the diplexer was included in the electrodynamic model. In the pass band of the five-resonator filter 1024–1036 MHz, the losses were in the center -0.47 dB, and at the edges of the band, respectively -0.61 and -0.58 dB (Fig. 8). For a four resonator filter in the center of the operating band 1084–1096 MHz, the losses are calculated to be -0.39 dB, and at the edges of the band -0.51, -0.41 dB. Thus, at the center of the diplexer operating bands, the insertion loss is approximately -0.4 dB, which meets the requirement of low insertion loss. This loss level was confirmed experimentally for a similar diplexer design with slightly changed operating frequency ranges, for which the calculated and experimental characteristics of the diplexer coincide.

To estimate the permissible maximum operating power of the diplexer in the electrodynamic model under study, a power of 2 kW was set at input 1 of the diplexer. The distribution of the electric field strength in the diplexer obtained at this value of the input power is shown in Fig. 9. As can be seen from the resulting distribution, the maximum value of the electric field strength is achieved in the gaps between the ends of the coaxial resonator and the top cover of the diplexer (red). According to calculations, $E_{\max} \cong 2.44 \cdot 10^6$ V/m, which is less than the known value of the breakdown electric field strength for air ($3 \cdot 10^6$ V/m). Consequently, this diplexer design allows operation at high power levels, which is required, for example, in radar systems. The proposed diplexer is characterized by compact dimensions ($132 \times 148 \times 35$ mm) and technological design, which is also well suited for the design of diplexers in various ranges of mobile and satellite communications. A comparison of the developed diplexer with well-known world analogues shows that in a number of characteristics (insertion loss, matching, power level) it is superior to analogues available on the market [20,21].

Conclusion

The work proposes an original design of an *L*-range diplexer based on coaxial resonators for high power operation, which is required, for example, in radar systems. The diplexer with operating bands 1024–1036/1084–1096 MHz is implemented on resonators with coaxial hollow mushroom-shaped cylinders. This form of coaxial cylinders ensures a significant reduction in the height of the resonant cavities and the diplexer as a whole. The diplexer contains an original matching circuit design based on *T*-coupling of stripline and coaxial lines.

The synthesis of the diplexer is carried out on the basis of an effective combined technique, including the use of coupling matrix apparatus, solving eigenproblems for a single and two coupled coaxial resonant cavities, synthesis of a matching circuit, electrodynamic modeling of channel filters and the diplexer as a whole using the finite element method. According to the results of electrodynamic modeling of the diplexer in the pass bands, the reflection coefficient does not exceed $S_{11} < -22$ dB, channel isolation $S_{32} = -70$ dB.

The insertion loss in the pass bands is $-0.4--0.6$ dB, the permissible input power level is 2 kW. The proposed diplexer design is technologically advanced, has compact dimensions and can be used to create diplexers for mobile and satellite communication systems. The reviewed synthesis technique can be used for various ratios of operating frequencies throughout the radio frequency and microwave ranges.

Conflict of interest

The authors declare that they have no conflict of interest.

References

[1] R.J. Cameron, C.M. Kudsia, R.R. Mansour. *Microwave Filters for Communication Systems: Fundamentals, Design and Applications* (Hoboken, NJ: Wiley, 2018)

[2] R.R. Mansour. *Proc. Radio and Wireless Conf. RAWCON'03.* (Boston, USA, 2003), p. 373–376, DOI: 10.1109/RAWCON.2003.1227970

[3] I.C. Hunter, L. Billonet, B. Jarry, P. Guillon. IEEE Transactions on Microwave Theory and Tech., **50** (3), 794 (2002). DOI: 10.1109/22.989963

[4] G. Macchiarella, S. Tamiazzo. IEEE Transactions on Microwave Theory and Tech., **58** (12), 3732 (2010). DOI: 10.1109/TMTT.2010.2086570

[5] P. Zhao, K.L. Wu. *IEEE MTT-S International Microwave Symposium (IMS2014)* (Tampa, FL, USA, 2014), p. 1–3, DOI: 10.1109/MWSYM.2014.6848399

[6] J.B. Thomas. IEEE Transactions on Microwave Theory and Tech., **51** (4), 1368 (2003). DOI: 10.1109/TMTT.2003.809180

[7] K. Kobrin, V. Rudakov, V. Sledkov, Z. Li, M. Manuilov. *Conf. Proc. Radiation and Scattering of Electromagnetic Waves (RSEMW-2019)*, (Divnomorskoe, Russia, 2019), p. 148–151, DOI: 10.1109/RSEMW.2019.8792810

[8] K.V. Kobrin, V.A. Rudakov, Z. Li, M.B. Manuilov. J. Electromagnetic. Waves Appl., **35** (2), 1273 (2021). doi.org/10.1080/09205071.2021.1886998

[9] K. Kobrin, V. Rudakov, Z. Li, V. Sledkov, M. Manuilov. *2020 7th All-Russian Microwave Conference (RMC-2020)*, (Moscow, Russia, 2020), p. 176–179, DOI: 10.1109/RMC50626.2020.9312259

[10] J.P. Venter, R. Maharaj, T. Stander. IEEE Trans. on Components, Packaging and Manufacturing Technol., **10** (4), 686 (2020). DOI: 101109/TCPMT.2020.2967807

[11] J. Li, G. Huang, T. Yuan, J. Xu, H. Li. *Proc. IEEE Intern. Symp. on Antennas and Propagation* (Boston, USA, 2018), p. 1439.

[12] S.J. Fiedziuszko, I.C. Hunter, T. Itoh, Y. Kobayashi, T. Nishikawa, S.N. Stitzer, K. Wakino. IEEE Transactions on Microwave Theory and Tech., **50** (3), 706 (2002). DOI: 10.1109/22.989956

[13] Z.C. Zhang, Q.X. Chu, S.W. Wong, S.F. Feng, L. Zhu, Q.T. Huang, F.-C. Chen. IEEE Trans. on Components, Packaging and Manufacturing Technol., **6** (3), 383 (2016). DOI: 10.1109/TCPMT.2016.2516820

[14] K.L. Wu. *Proc. Asia Pacific Microwave Conf. APMC 2012.* (Kaohsiung, Taiwan., 2012), p. 388–390, DOI: 10.1109/APMC.2012.6421607

[15] L. Pelliccia, F. Cacciamani, A. Cazzorla, D. Tiradossi, P. Vallerotonda, R. Sorrentino, W. Steffè, F. Vitulli, E. Picchione, J. Galdeano, P. Martìn-Igleasias. *Proc. 49th European Microwave Conf.* (Paris, France, 2019), p. 61–64, DOI: 10.23919/EuMC.2019.8910684

[16] V. Rudakov, V. Sledkov, Z. Li, V. Taranenko, M. Manuilov. *Proc. 2023 Radiation and Scattering of Electromagnetic Waves, RSEMW 2023*, (Divnomorskoe, Russia, 2023), p. 80–83, DOI: 10.1109/RSEMW58451.2023.10202146

[17] M.B. Manuilov, K.V. Kobrin. Radiophys. Quant. Electron., **59** (4), 301 (2016). DOI: 10.1007/s11141-016-9698-2

[18] G. L. Matthaei, L. Young, M. T. Jones. *Microwave Filters, Impedance-Matching Networks, and Coupling Structures.* New York: McGraw-Hill, vol. 2, 1964

[19] Electronic media. ANSYS Electromagnetics Suite. Available at: https://www.ansys.com

[20] Electronic media. Available at: http://cernexwave.com/filters-diplexers-2/

[21] Electronic media. Available at: https://rlcelectronics.com/products/filters/high_power_and_standard_cellular_duplexers/

Translated by A.Akhtyamov